Received: 23 June 2022 | Revised: 8 November 2022 | Accepted: 9 November 2022

DOI: 10.1002/mgg3.2108

Molecular Genetics & Genomic Medicine Open Access WILEY

ORIGINAL ARTICLE

A novel splicing mutation in 5′UTR of GJB1 causes X-linked Charcot—Marie–tooth disease

MeiYi Li[1] | Minna Yin[1] | Li Yang[1] | Zhiheng Chen[1] | Peng Du[2] | Ling Sun[1] | Juan Chen[1]

[1]Center of Reproductive Medicine, Guangzhou Women and Children's Medical Center, Guangzhou Medical University, Guangzhou, China

[2]Genetic Testing Center, Guangzhou Women and Children's Medical Center, Guangzhou Medical University, Guangzhou, China

Correspondence
Juan Chen and Ling Sun, Center of Reproductive Medicine, Guangzhou Women and Children's Medical Center, Guangzhou Medical University, Guangzhou, Guangdong 510623, People's Republic of China.
Email: chenjuan91@hotmail.com and sunling6299@163.com

Funding information
National Natural Science Foundation of China, Grant/Award Number: 81800110

Abstract

Background: Charcot–Marie–Tooth (CMT) disease is the most frequent hereditary motor sensory neurological disease. GJB1 gene is the second most frequent cause of CMT, accounting for approximately 10% of CMT cases worldwide. We identified a large Han family with X-linked CMT disease.

Methods: In this study, the probands and his mother underwent electrophysiological examinations and other family members were assessed retrospectively. Whole-exome sequencing, Sanger sequencing, and SNP array linkage analysis were performed to find and confirm the variant. The functional effect of the identified variant was further investigated in HEK293 cells and MCF-7 cells by minigene splicing assay.

Results: The affected individuals had some clinical symptoms including symmetric atrophy and progressive weakness of the distal muscles in their twenties. Electrophysiological examinations result in peripheral nerve injury of the upper and lower limbs. Whole-exome sequencing identified a novel hemizygous deletion mutation (NM_000166: c.-16-8_-14del) in the GJB1 gene. SNP array linkage analysis and co-segregation analysis confirmed this mutation. Minigene splicing assay verified that this mutation leads to the activation of cryptic splicing sites in exon 2 which results in the deletion of exon 2.

Conclusion: Our study provides theoretical guidance for prenatal diagnosis and subsequent fertility of this family. This result expands the spectrum of mutations in GJB1 known to be associated with CMTX and contributes to the diagnosis of CMT and clinical genetic counseling.

KEYWORDS
Charcot–Marie–tooth disease, genetic counseling, GJB1, novel mutation

1 | INTRODUCTION

Charcot–Marie–Tooth disease (CMT) is the most frequent hereditary motor sensory neurological disease with an estimated prevalence of 1/2500 in the population (Barreto et al., 2016; Hoyle et al., 2015). CMT disease exhibits considerable clinical heterogeneity and it is characterized by progressive muscular weakness, foot deformities, gait

disturbance, absence of reflexes, distal muscle atrophy, and sensory impairment (Pareyson et al., 2017). On the basis of electrophysiologic properties and histopathology, CMT can be further classified into the demyelinating type (CMT1), the axonal defective type (CMT2), and intermediate type (DI-CMT), which is characterized by demyelination and axonal loss (Morena et al., 2019). To date, more than 90 causative genes have been associated with CMT. Despite significant genetic heterogeneity, PMP22, GJB1, MPZ, and MFN2 are the most common genes responsible for CMT disease (Sun et al., 2019).

X-linked Charcot–Marie–Tooth disease (CMTX) is the second most common cause of CMT, accounting for 10%–20% of all CMT cases (Liu et al., 2020). According to previous reports, CMTX is mostly caused by mutations in the gene GJB1 encoding the gap junction protein Connexin 32 (Cx32), a gap junction protein localized to the paranodal regions and incisures of myelinating Schwann cells (Brewer et al., 2010). Human GJB1 consists of two exons. Exon 1 encodes most of the 5′ untranslated region (UTR). Exon 2 contains the entire amino acid coding region and the 3′UTR. Two different transcripts (NM_000166.6 and NM_001097642.3) are regulated by two different tissue-specific promoters (P1 and P2). Promoter P1 locates at about 8 kb upstream from the coding sequence and regulates the expression of transcript NM_001097642 in the liver, pancreas, oocytes, and embryonic stem cells. Promoter P2 positions in intron 1 of transcript NM_001097642 and is responsible for the expression of the transcript NM_000166.6 in the peripheral nervous system. Though these two different transcripts include different 5′UTR, they provide mRNAs with identical coding regions(Boso et al., 2020). To date, most of the known variants are in the coding region, with the majority being missense mutations and rarer cases with frameshift and premature stop codon mutations or ample deletions. Thanks to the broader availability of genetic screening, recent research reported that the noncoding region of GJB1 is the key regulator of protein expression and mutations in this region are the major cause of X-linked CMT, accounting for 10% of patients with GJB1 mutations (Boso et al., 2020; Tomaselli et al., 2017). Recent research reported that variations of the UTR may become pathogenic by disrupting the sequences that regulate transcription or by impairing mRNA translation and stability, thus influencing protein expression. The study also raises the possibility that variations of the UTR may be a more frequent cause of other inherited neurologic conditions than has been previously appreciated to cause recessive disease (Tomaselli et al., 2017). Here we report a large family presented with an adult-onset, slowly progressive, axonal defective CMT. Molecular and genetic investigation of the GJB1 gene revealed a novel splicing mutation that is predicted to result in the deletion of exon2.

2 | MATERIALS AND METHODS

2.1 | Patients and clinical examination

A large Han family with X-linked CMT disease was identified when the proband came to Guangzhou Women and Children's Medical Center for genetic counseling. The proband and his mother received complete neurological examinations by neurologists based on the clinical guidelines of the European CMT consortium. All procedures in this study were approved by the Reproductive Medical Ethics Committee of Guangzhou Women and Children's Hospital. Written informed consent was obtained from all participants or their guardians before enrolment in this study.

2.2 | Whole exome sequencing

Genomic DNA was obtained from the peripheral blood leukocytes of 15 family members using a Fast Pure Blood DNA Isolation Mini Kit (Vazyme) according to the instructions.

Whole-exome sequencing (WES) was performed for the proband (IV-5) by the GenCap® Full Exon Gene Capture Probe V4.0 and a HiSeq 2000 Genome Analyzer (Illumina) with 100-bp paired-end reads. UCSC assembly GRCh37/hg19 was used as the reference sequence. Available genomic databases (dbSNP, 1000 Genomes Project, EXAC the Exome Aggregation Consortium, ESP6500 NHLBI Exome Sequencing Project, and a local Paris Descartes Bioinformatics platform database) were used to filter exome variants and exclude variants with a frequency >1%. We first filtered out the intronic variants and synonymous single-nucleotide variants. Then, we removed the variants annotated in dbSNP without pathogenic relevance to the clinical phenotype. Poor quality variants were excluded (read depth <30; alternative variant frequency <5).

2.3 | SNP array linkage analysis

Three hundred and twenty six SNP markers located 5 Mb upstream and downstream of the mutation site (GRCh38, chrX:g.71223684_71223694del) were chosen for NGS-based SNP haplotyping and SNP primers of these SNP markers were designed by Ion Ampliseq Designer (https://www.ampliseq.com/). Genomic DNA library of 13 family

members was constructed using these SNP primers and NGS was performed for both SNP haplotyping and mutation locus analysis. Sequencing libraries were prepared using the gene sequencing library kit (NEXTflex Rapid DNA-seq Kit 96rxns, BIOO), and libraries were sequenced on an Illumina MiseqDX platform (Illumina) using MiSeq Dx Reagent Kit V3 (Illumina). All of the procedures were carried out in accordance with the manufacturer's protocol. The sequencing data were analyzed by Peking Jabrehoo Med Tech., Ltd. Of the 326 SNPs, 189 informative SNPs including the pathogenic mutation site were selected to establish the haplotype and distinguish the mutant/affected haplotype.

2.4 | Family co-segregation analysis

All candidate variants were confirmed by PCR and direct Sanger sequencing using the DNA of all patients. The primers for amplifying the GJB1 variant were as follows: forward: 5′-TAGGGGACAGGGAGCCATAG-3′ and reverse: 5′-AGAGCCATACTCGGCCAATG-3′.

2.5 | Bioinformatics

To further confirm the effect of mutation on the splicing of GJB1, the variant was predicted using three bioinformatics databases, Mutation Taster (http://www.mutationtaster.org/), Splice Site Prediction by Neural Network (http://www.fruitfly.org/seq_tools/splice.html) and GnomAD (https://gnomad.broadinstitute.org/about?tdsourcetag=s_pctim_aiomsg).

2.6 | Minigene plasmids construct

GJB1 wild type (WT) and mutant type (MUT) gene sequences were amplified from peripheral blood leukocytes genomic DNA of IV-7 and IV-4, respectively. The primers for constructing pcMINI-C-GJB1-WT/MUT plasmids were as follows: forward primer(pcMINI-C-GJB1-KpnI-F): 5′-ggtaGGTACCttggatgaaagcgaagaagg-3′ and reverse primer(pcMINI-C-GJB1-BamHI-R): 5′-TAGTGGATCCtcagcaggccgagcagcggt-3′. As for pcDNA3.1-GJB1-WT/MUT plasmids, forward primer(pcDNA3.1-GJB1-KpnI-F): 5′-GCTTGGTACCATGGGGCGGTGATGAATTGGGAC-3′ and reverse primer(pcDNA3.1-GJB1-BamHI-R): 5′-TAGTGGATCCtcagcaggccgagcagcggt-3′ were used. Amplification products were subsequently cloned into pcMINI-C or pcDNA3.1 expression vector by double digestion with KpnI and BamHI enzyme (New England Biolabs). Recombinant plasmids were purified with the Endo-Free Plasmid Midi Kit (Omega Bio-Tek) and confirmed by Sanger sequencing.

2.7 | Minigene splicing assay

HEK293T cells and MCF-7 cells were cultured in six-well dishes at 37°C in a 5% CO_2 atmosphere in a sterile incubator (Thermo Fisher Scientific). DMEM (Invitrogen) supplemented with 10% FBS (GIBCO, Thermo Fisher Scientific) was used for cell culture. Cells were transfected with 2 μg of pcMINI-C-GJB1-WT/MUT or pcDNA3.1-GJB1-WT/MUT recombinant plasmid. After a further 24 h culture, cells were collected and lysed in Trizol (Thermo Fisher Scientific). The total RNA was extracted and reverse-transcribed to cDNA using the Go Script Reverse Transcription System (Promega). Primers on both sides of the minigene were used for PCR amplification, agarose was used to detect the size of gene transcription bands, and sequencing was performed.

3 | RESULTS

3.1 | Patient phenotypes

A large Han family with X-linked CMT disease was identified when the proband came to Guangzhou Women and Children's Medical Center for genetic counseling. Due to hand tremors and thenar muscle atrophy, he previously went to the hospital for treatment and was diagnosed with CMT after receiving complete neurological examinations based on the clinical guidelines of the European CMT consortium (Table 1). Because his wife was pregnant with twins, he came to our hospital for genetic counseling and hope to find out the disease-causing gene. Clinical features information was collected from the proband and other affected individuals (Table 2). The proband was onset at an early age with the clinical symptoms of thenar muscle atrophy. He found it hard to hold a pen with hand tremors and cramps. It got worse as he got older with running difficulties caused by calf muscular atrophy and foot deformity. Two male patients (III-1; III-5 in Figure 1c) had similar onset age and severity as the proband. They lost the ability to run around the age of 30. As the disease progresses, both cases presented with walking difficulties, sensory abnormalities, and slowly progressive distal muscle weakness with peroneal atrophy and foot deformities now. Two patients (III-10; IV-9 in Figure 1c) presented with more serious clinical symptoms. Female patients behaved with milder symptoms including calf muscular atrophy and mild walking difficulties.

TABLE 1 Electrodiagnostic findings in the proband and his mother

	III-7		IV-5	
CMAP (mV)/MCV (m/s)	**Left**	**Right**	**Left**	**Right**
Motor nerve conduction				
Median nerve	45.8/9.3	NC	35.0/3.0	20.0/0.5
Ulnar nerve	43.9/7.9	NC	34.0/3.8	35.0/6.3
Posterior tibial nerve	NC	32.2/3.0	28.0/0.3	18/0.1
Deep peroneal nerve	NC	33.9/0.4	NR	NR
Sensory nerve conduction				
Median nerve	26.5/2.5	NC	30.0/2.0	29.0/1.0
Ulnar nerve	28.5/2.6	NC	NR	NR
Superficial peroneal nerve	NR	NC	NR	NR
Radial nerve	27.7/3.1	NC	NC	NC
Sural nerve	NC	27.5/3.5	NR	NR
Medial plantar nerve	NC	NR	NC	NC

Abbreviations: CMAP, compound muscle action potential; MCV, motor conduction velocities; NR, no response; NC, no record.

TABLE 2 Clinical features of the affected individuals with Charcot–Marie–tooth disease

	III-1	III-5	III-7	III-10	III-11	IV-5	IV-9
Gender	M	M	F	M	F	M	M
Age	65	60	56	58	60	29	33
Initial symptom	Difficulty walking	Difficulty walking	asymptomatic	Distal leg weakness	Impossible to run	Impossible to run	Impossible to walk quickly
Muscle weakness	DLL > DUL	DLL > DUL	DLL > DUL	DLL > DUL	DLL > DUL	DLL = DUL	DLL > DUL
Muscle atrophy	Yes	Yes	Yes	Yes	Yes	Yes	Yes
Deformity	Pes cavus	Pes cavus	No	Pes cavus	No	Pes cavus	Pes cavus

Abbreviations: DLL, distal lower limbs; DUL, distal upper limbs.

3.2 | Mapping and identification of GJB1 mutation

To identify the underlying genetic defects, whole exome sequencing of the proband was performed. According to the mutation frequency and human genomic database, 54 candidate genes were found. Three of them best matched with clinical symptoms of this family. Sanger sequencing (Figure 1b) found that the GJB1 deletion mutation (NM_000166: c.-16-8_-14del) co-segregated with the CMT phenotype in the family members. The other two variants are FIG4 NM_014845 c.1165A>G and SYT2 NM_1774 02 c.919+4C>T, variant of FIG4 fulfilled criterion PM2, BP4, and the variant of SYT2 fulfilled criterion BS2, and both classified as uncertain significance according to ACMG. These two variants did not co-segregated with the CMT phenotype in the family members and, therefore, were excluded.

3.3 | NGS-based SNP haplotyping

We analyzed the genotypes of the SNP alleles of 326 SNP sites from the gDNA of 13 family members using NGS. Based on the heterozygote SNPs in the female III-9, we selected homozygote or heterozygote SNPs for the III-10 and IV-7 at the same loci to construct the pedigree haplotypes. A total of 189 informative SNP sites were chosen to construct the pedigree haplotypes to distinguish the chromosome of the GJB1 gene. Based on the pedigree haplotypes, all the patients carry the same chromosome with GJB1 mutation (verification by Sanger Sequencing) (Figure 2a,b).

3.4 | Bioinformatics prediction and minigene splicing assay

To further confirm the splicing mutation of GJB1, biogenetic analysis was performed by Mutation Taster (http://www.mutationtaster.org/) and BDGP: Splice Site Prediction by Neural Network (http://www.fruitfly.org/seq_tools/splice.html). Both Mutation Taster and BDGP: Splice Site Prediction by Neural Network suggested that small deletion mutation (NM_000166: c.-16-8_-14del) in GJB1 located at the exon-intron junction and might alter the splice site. To evaluate the effect of the mutation,

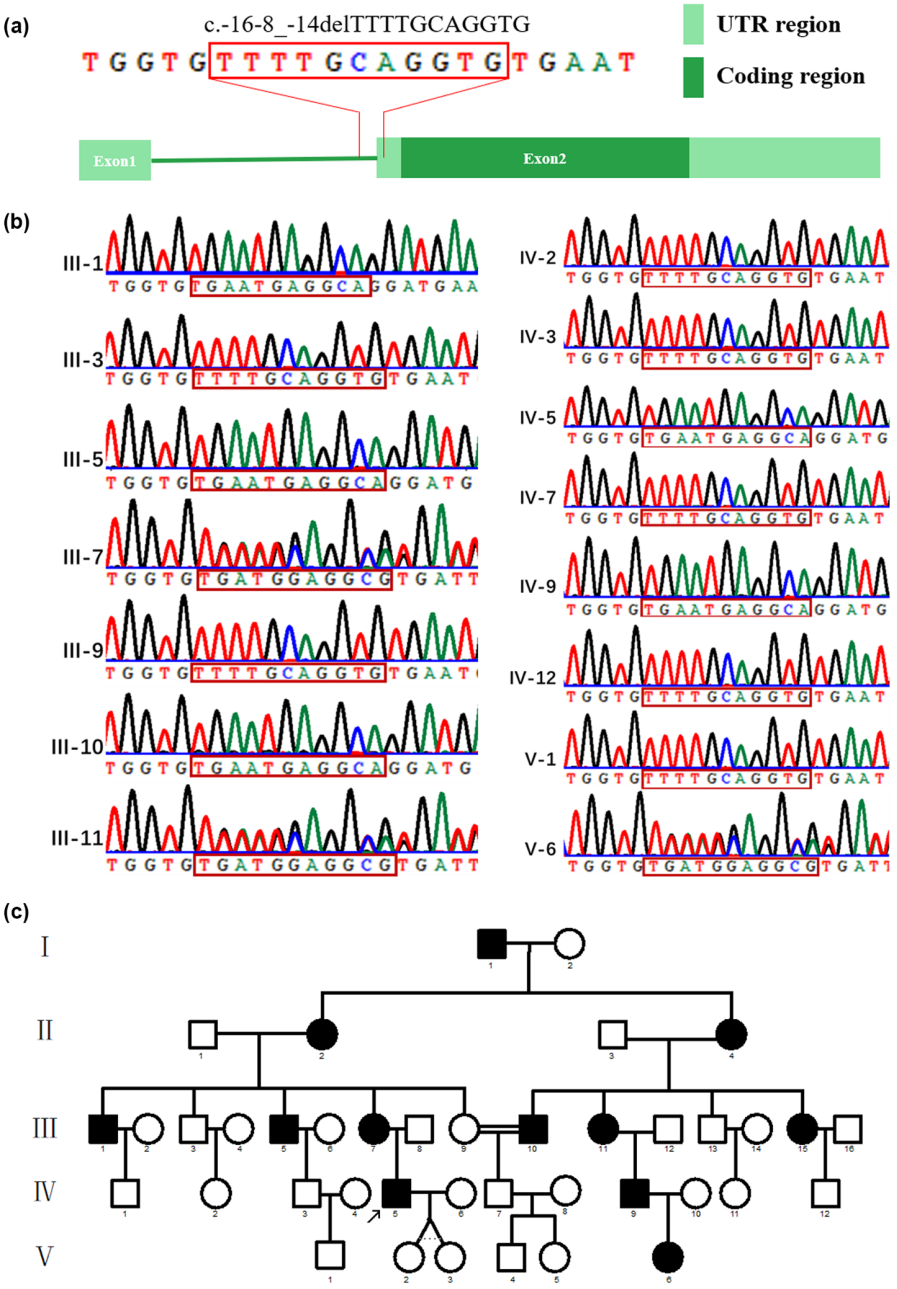

FIGURE 1 Causative variant detection in this family. (a) A map of the gene location of this mutation. (b) Sanger sequencing result and co-segregation analysis of the mutation GJB1(NM_000166: c.-16-8_-14del). All the patients in this family carry this mutation. (c) Pedigree of the CMT disease family reported in this study.

Minigene splicing assay was performed. Recombinant plasmids pcDNA3.1-GJB1-WT/MUT or pcMINI-C-GJB1-WT/MUT were constructed and transfected in HEK 293T cells or MCF-7 cells, respectively. PCR, electrophoresis, and direct sequencing suggested that the mutation in both pcMINI-C-GJB1 and pcDNA3.1-GJB1 plasmids lead to the activation of cryptic splicing sites in exon 2 and a deletion of 278 bp of exon 2, which contains the physiological ATG initiation site of CX32 (Figure 3a,b,d,e). A different in-frame ATG may be used, leading to a shorter protein lacking 92 amino acids at the N-terminus (Figure 3c,f). In addition, the mutation in pcMINI-C-GJB1 plasmid can also lead to the activation of cryptic splicing sites in exon 2 and a deletion of 545 bp of exon 2 (Figure 3e). By cloning the band B into a T vector and sequencing, the mutation in pcDNA3.1-GJB1 plasmid can also lead to the activation of cryptic splicing sites in exon 2 and a deletion of 256 bp of exon 2 (Figure 3b). Although there were two splicing modes of band b, the deletion of 278 bp was the main splicing mode according to PCR product sequencing.

4 | DISCUSSION

Mutations in the GJB1 gene are the second most frequent cause of CMT, accounting for approximately 10% of CMT cases worldwide (Gouvea et al., 2019). There are

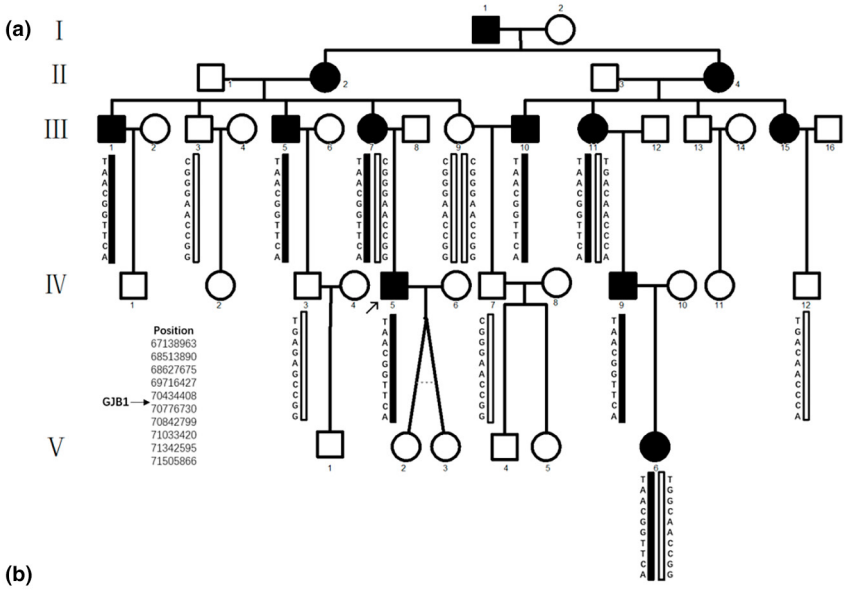

(b)

Position	III-1 F0	III-3 M1	III-5 F0	III-7 M0	III-7 F0	III-9 M0	III-9 M1	III-10 F0	III-11 F0		IV-3	IV-5 F0	IV-7 M1	IV-9 F0	IV-12	V-6 F0	
70263784	C	T	C	C	C	C	T	C	C	C	T	C	T	C	C	C	C
70268533	G	A	G	G	G	G	A	G	G	G	A	G	A	G	G	G	G
70275832	A	?	G	A	A	A	C	A	A	A	C	A	C	A	A	A	A
70292200	G	A	G	G	G	G	A	G	G	T	A	G	A	G	G	G	G
70321631	T	T	T	G	T	G	T	T	T	T	T	T	T	T	T	T	G
70330596	T	T	T	C	T	C	T	T	T	T	T	T	T	T	T	T	C
70338399	A	A	A	G	A	G	A	A	A	A	A	A	A	A	A	A	G
70351838	C	C	C	T	C	T	C	C	C	C	C	C	C	C	C	C	T
70356642	T	T	T	C	T	C	T	T	T	T	T	T	T	T	T	T	C
70371574	T	T	T	G	T	G	T	T	T	T	T	T	T	T	T	T	G
70400555	T	T	T	C	T	C	T	T	T	T	T	T	T	T	T	T	C
70401585	T	T	T	C	T	C	T	T	T	T	C	T	T	T	T	T	C
70404639	A	G	A	A	A	A	G	A	A	G	G	A	G	A	G	A	A
70412479	A	?	A	A	A	A	G	A	A	G	A	A	G	A	G	A	A
70434408	G	A	G	A	G	A	A	G	G	A	A	G	A	G	A	G	A
70457083	A	A	A	T	A	T	A	A	A	T	A	A	A	A	T	A	A
70543355	T	T	T	G	T	G	T	T	T	G	G	T	T	T	G	T	G
70746572	A	?	A	A	A	A	G	A	A	G	A	A	G	A	G	A	G
70754534	A	G	A	A	A	A	G	A	A	G	A	A	G	A	G	A	G
70773786	C	?	C	A	C	A	A	C	C	A	C	C	A	C	A	C	A
70776730	G	A	G	A	G	A	A	G	G	A	G	G	A	G	A	G	A
70780432	G	?	G	A	G	A	A	G	G	A	G	G	A	G	A	G	A
70842799	T	C	T	C	T	C	C	T	T	C	C	T	A	T	C	T	C
70851919	T	G	T	G	T	G	G	T	T	G	G	T	G	T	G	T	G
70851920	C	T	C	C	C	C	T	C	C	C	C	C	T	C	C	C	C
70855518	C	T	C	C	C	C	T	C	C	C	C	C	T	C	C	C	C
71024480	G	G	G	A	G	A	G	G	G	A	A	G	G	G	A	G	A
71033420	T	C	T	C	T	C	C	T	T	C	C	T	C	T	C	T	C
71051047	C	?	C	A	C	A	C	C	C	A	C	C	C	C	A	C	A
71064268	C	?	C	G	C	G	G	C	C	G	G	C	G	C	G	C	G

an unaffected haplotype an unaffected haplotype an unaffected haplotype

an affected haplotype

FIGURE 2 Family pedigree and pedigree-based linkage analysis and NGS-based SNP haplotyping results. (a) Family pedigree and pedigree-based linkage study of affected and unaffected individuals. The segregating haplotype is indicated by 326 SNP markers located 5 Mb upstream and downstream of the mutation site. GJB1 is flanked by positions 70434408 and 70776730. Affected subjects are denoted in black. The proband is indicated by an arrow. The reference genome was GRCH37/ HG19. (b) NGS-based SNP haplotyping results of 13 family members. 189 informative polymorphic SNP markers located upstream and downstream of the mutation site in GJB1 were selected to establish the haplotype. The positions marked in dark green color are informative SNPs for III-10 while the positions in light green are for III-9. The black line between positions 70434408 and 70776730 represent the mutation sites. III-1, III-5, III-10, IV-5, and IV-9 exhibited an affected haplotype pattern (F0).

two transcriptions of GJB1 regulated by 2 tissue-specific promoters (P1 and P2), allowing differential expression of these transcripts in neuronal and non-neuronal tissue (Piechocki et al., 2000). For neuronal tissues, it is regulated by the P2 promoter. To date, 459 mutations of the GJB1 gene identified as disease-causing have been recorded in the HGMD database (http://www.hgmd.cf.ac.uk/ac/search.php), only 5 (NM_000166: c.-16–12-16-2del, c.-16-3C>G, c.-16-2A>G, c.-17+1G>T,c.-17G>A) (Benedetti et al., 2010; Tomaselli et al., 2017; Xie et al., 2021) of them are splicing mutations. But recent research reported that mutations in noncoding regions of GJB1 were a major cause of X-linked CMT (Tomaselli et al., 2017). For the patients in whom Sanger sequencing of the coding region of GJB1 was negative, further screening of the 5′ and 3′UTR found pathogenic mutations.

In our study, we found a novel deletion mutation in the 5′UTR region of GJB1 (NM_000166: c.-16-8_-14del) fulfilled criterion PM2, PP3 and was classified as Class 3 (Uncertain Significance) according to the American College of Medical Genetics and Genomics (ACMG) criteria (Karczewski et al., 2020). Based on the linkage analysis and co-segregated result, this mutation fulfilled criterion PM2, PP1-M, PP3, PP4, and was classified as Class 5 (pathogenic). Further minigene splicing assay verified that this mutation produced two new splice variants (resulted in the deletion of the first 256/278/545 nucleotides of exon 2) that were likely to be translated into truncated protein. This result fulfilled

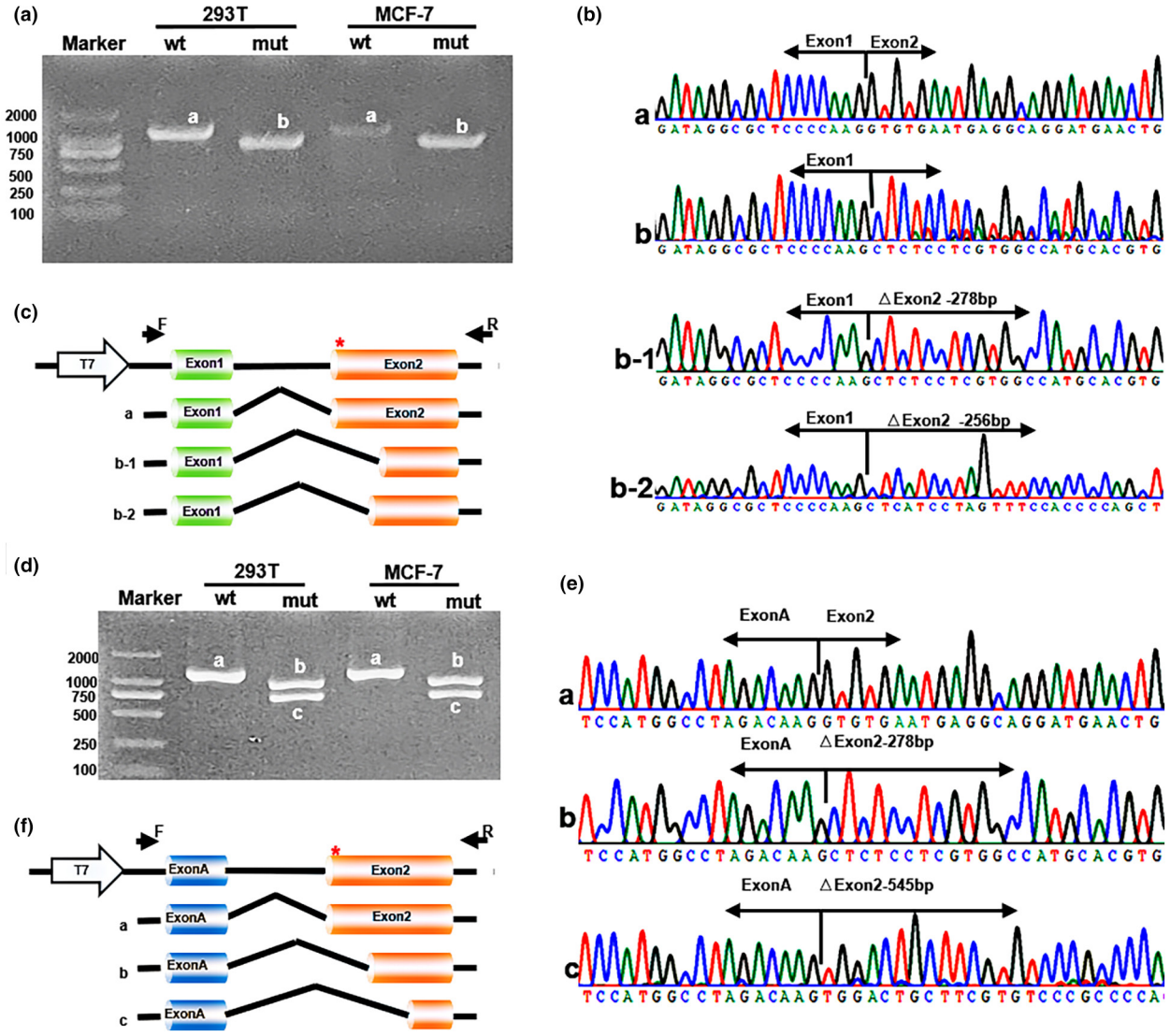

FIGURE 3 Minigene splicing assay result. (a) RT-PCR transcriptional analysis runs glue map of pcDNA3.1-GJB1-WT/MUT. (b) Sanger sequence results of bands in a. (c) Minigene construction strategy of pcDNA3.1-GJB1-WT/MUT. (d) RT-PCR transcriptional analysis runs glue map of pcMINI-C-GJB1-WT/MUT. (e) Sanger sequence results of bands in D. (f) Minigene construction strategy of pcMINI-C-GJB1-WT/MUT.Red * indicates the mutation location.

the ACMG criterion of PS3. Likewise, Benedetti et al. proved that a c.-16-3C>G substitution activated a cryptic splice site which resulted in the deletion of the first 278 nucleotides of exon 2, which consisted of part of our result (Benedetti et al., 2010). However, it was previously reported that the change of the canonical splice site sequence (c.-17+1G>T) causes the retention of the whole intron 1 into the mRNA and demonstrated a 70% reduction of the transcript level of GJB1 expression (Boso et al., 2020). When compared to this report, our patients also had fairly typical clinical, neurophysiological and pathological features, bearing a phenotype that co-segregated with the variant. The difference is that our mutation causes a 278 bp truncated mRNA, while the reported mutation (c.-17+1G>T) causes a transcript that was 356 bp longer than the mRNA of a control nerve biopsy, ultimately resulting in reduced protein expression of Cx32.

With the development of sequencing technology, next-generation sequencing (NGS) is increasingly being used in clinical diagnosis. Although there is a desire to use NGS as a single method to detect all clinically relevant genetic changes, especially for inherited diseases, the ability to interpret all of those data lags. The knowledge of how to interpret novel or rare mutations is still limited (Yohe & Thyagarajan, 2017). The pathogenicity of mutations needs to be judged with particular caution in clinical genetics counseling for such patients. In our study, the proband went to our center for genetics counseling for his unborn twins. Through a series of experiments, we identified this mutation as a pathogenic mutation and upgraded the pathogenicity rating according to the ACMG criteria. Unfortunately, both twins carry

this disease-causing mutation. Considering female patients demonstrate milder symptoms, just the mother (III-7), he ultimately decided to keep the twins.

In conclusion, we demonstrated that the novel candidate variant of GJB1(c.-16-8_-14del11) does cause CMTX. The mutation co-segregates with typical clinical phenotype in a large Chinese pedigree and is located in a highly conserved position, at the interface between intron 1B and exon 2, similar to other adjacent putative causative variants, thus emphasizing its functional importance. Our results expand the spectrum of mutations in GJB1 known to be associated with CMTX and contribute to the diagnosis of CMT and clinical genetic counseling.

AUTHOR CONTRIBUTIONS

Meiyi Li performed experiments, analyzed the data, prepared tables and figures, and wrote the manuscript. Minna Yin, Li Yang, Zhiheng Chen, and Peng Du interpreted the data, and edited the manuscript. Ling Sun and Juan Chen designed the study, supervised the interpretation and statistical analysis of the data, and edited the manuscript. All the authors approved the final version of the manuscript.

ACKNOWLEDGMENTS

This study is supported by the National Natural Science Foundation of China (81800110).

CONFLICT OF INTEREST

The authors declare no competing financial interests.

DATA AVAILABILITY STATEMENT

The data used to support the findings of this study are available from the corresponding author upon request.

ORCID

MeiYi Li https://orcid.org/0000-0003-2286-198X
Peng Du https://orcid.org/0000-0002-8730-8520

REFERENCES

Barreto, L. C., Oliveira, F. S., Nunes, P. S., de Franca Costa, I. M., Garcez, C. A., Goes, G. M., Neves, E. L., de Souza Siqueira Quintans, J., & de Souza Araujo, A. A. (2016). Epidemiologic study of Charcot-Marie-tooth disease: A systematic review. *Neuroepidemiology*, *46*, 157–165.

Benedetti, S., Previtali, S. C., Coviello, S., Scarlato, M., Cerri, F., Di Pierri, E., Piantoni, L., Spiga, I., Fazio, R., Riva, N., Natali Sora, M. G., Dacci, P., Malaguti, M. C., Munerati, E., Grimaldi, L. M., Marrosu, M. G., De Pellegrin, M., Ferrari, M., Comi, G., … Bolino, A. (2010). Analyzing histopathological features of rare charcot-marie-tooth neuropathies to unravel their pathogenesis. *Archives of Neurology*, *67*, 1498–1505.

Boso, F., Taioli, F., Cabrini, I., Cavallaro, T., & Fabrizi, G. M. (2020). Aberrant splicing in GJB1 and the relevance of 5′UTR in CMTX1 pathogenesis. *Brain Sciences*, *11*, 24.

Brewer, M. H., Chaudhry, R., McDowall, K., Chu, S., Kowalski, B., Polly, P., Nicholson, G., & Kennerson, M. (2010). X-linked CMT: Genes and gene loci in an Australian cohort. *Neurogenetics*, *11*, 267–269.

Gouvea, S. P., Tomaselli, P. J., Barretto, L. S., Perina, K. C. B., Nyshyama, F. S., Nicolau, N., Jr., Lourenco, C. M., & Marques, W., Jr. (2019). New novel mutations in Brazilian families with X-linked Charcot-Marie-tooth disease. *Journal of the Peripheral Nervous System*, *24*, 207–212.

Hoyle, J. C., Isfort, M. C., Roggenbuck, J., & Arnold, W. D. (2015). The genetics of Charcot-Marie-tooth disease: Current trends and future implications for diagnosis and management. *The Application of Clinical Genetics*, *8*, 235–243.

Karczewski, K. J., Francioli, L. C., Tiao, G., Cummings, B. B., Alfoldi, J., Wang, Q., Collins, R. L., Laricchia, K. M., Ganna, A., Birnbaum, D. P., Gauthier, L. D., Brand, H., Solomonson, M., Watts, N. A., Rhodes, D., Singer-Berk, M., England, E. M., Seaby, E. G., Kosmicki, J. A., … MacArthur, D. G. (2020). The mutational constraint spectrum quantified from variation in 141,456 humans. *Nature*, *581*, 434–443.

Liu, Y., Xue, J., Li, Z., Linpeng, S., Tan, H., Teng, Y., Liang, D., & Wu, L. (2020). A novel GJB1 mutation associated with X-linked Charcot-Marie-tooth disease in a large Chinese family pedigree. *Molecular Genetics & Genomic Medicine*, *8*, e1127.

Morena, J., Gupta, A., & Hoyle, J. C. (2019). Charcot-Marie-tooth: From molecules to therapy. *International Journal of Molecular Sciences*, *20*, 3419.

Pareyson, D., Saveri, P., & Pisciotta, C. (2017). New developments in Charcot-Marie-tooth neuropathy and related diseases. *Current Opinion in Neurology*, *30*, 471–480.

Piechocki, M. P., Toti, R. M., Fernstrom, M. J., Burk, R. D., & Ruch, R. J. (2000). Liver cell-specific transcriptional regulation of connexin32. *Biochimica et Biophysica Acta*, *1491*, 107–122.

Sun, S. C., Ma, D., Li, M. Y., Zhang, R. X., Huang, C., Huang, H. J., Xie, Y. Z., Wang, Z. J., Liu, J., Cai, D. C., Liu, C. X., Yang, Q., Bao, F. X., Gong, X. L., Li, J. R., Hui, Z., Wei, X. F., Zhong, J. M., Zhou, W. J., … Xu, X. M. (2019). Mutations in C1orf194, encoding a calcium regulator, cause dominant Charcot-Marie-tooth disease. *Brain*, *142*, 2215–2229.

Tomaselli, P. J., Rossor, A. M., Horga, A., Jaunmuktane, Z., Carr, A., Saveri, P., Piscosquito, G., Pareyson, D., Laura, M., Blake, J. C., Poh, R., Polke, J., Houlden, H., & Reilly, M. M. (2017). Mutations in noncoding regions of GJB1 are a major cause of X-linked CMT. *Neurology*, *88*, 1445–1453.

Xie, Y., Lin, Z., Liu, L., Li, X., Huang, S., Zhao, H., Wang, B., Zeng, S., Cao, W., Li, L., Zhu, X., Huang, S., Yang, H., Wang, M., Hu, Z., Wang, J., Guo, J., Shen, L., Jiang, H., … Zhang, R. (2021). Genotype and phenotype distribution of 435 patients with Charcot-Marie-tooth disease from central South China. *European Journal of Neurology*, *28*, 3774–3783.

Yohe, S., & Thyagarajan, B. (2017). Review of clinical next-generation sequencing. *Archives of Pathology & Laboratory Medicine*, *141*, 1544–1557.

How to cite this article: Li, M., Yin, M., Yang, L., Chen, Z., Du, P., Sun, L., & Chen, J. (2023). A novel splicing mutation in 5′UTR of GJB1 causes X-linked Charcot—Marie–tooth disease. *Molecular Genetics & Genomic Medicine*, *11*, e2108. https://doi.org/10.1002/mgg3.2108